

# Chemistry–A European Journal

Supporting Information

## **A Combined Spectroscopic and Theoretical Study on a Ruthenium Complex Featuring a $\pi$ -Extended dppz Ligand for Light-Driven Accumulation of Multiple Reducing Equivalents**

Carolin Müller,\* Alexander Schwab, Nicholas M. Randell, Stephan Kupfer,\* Benjamin Dietzek-Ivanšić,\* and Murielle Chavarot-Kerlidou\*

1 Experimental and computational absorption data .....	2
1.1 Ru.....	2
1.2 RuH <sup>+</sup> .....	5
1.3 RuH <sub>2</sub> .....	12
2 Resonance Raman Spectra .....	15
3 Steady-state and time-resolved emission spectra .....	16
4 Time-resolved emission and transient absorption data.....	17
4.1 Characterization of the long-lived excited state .....	17
4.2 Photoinduced dynamics .....	17

## 1 Experimental and computational absorption data

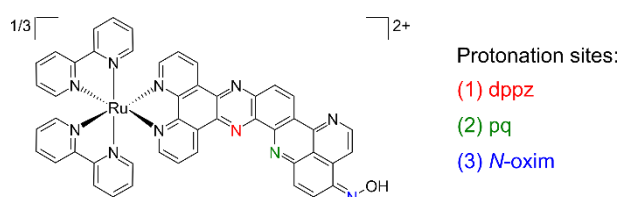


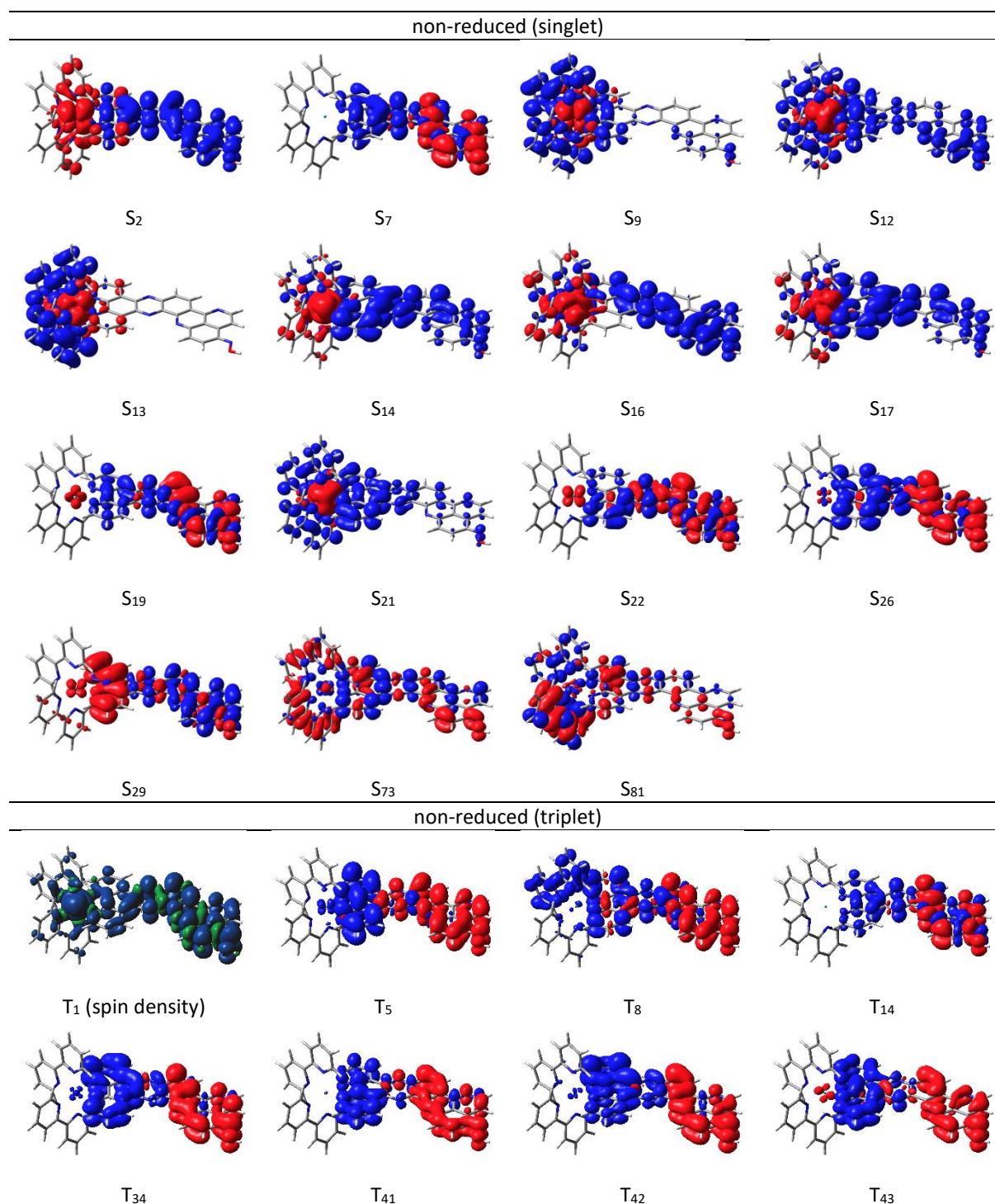
**Figure S1.** Computationally assessed redox and protonation states of **Ru**; both singlet and triplet multiplicity were considered for all intermediates. Three singly-protonated species with protonation (**RuH<sup>+</sup>**) occurring at dipyrrophenazine (dppz, in red) vs. pyridoquinolinone (pq, in green) vs. N-oxime (in blue) were investigated. Further, three doubly-protonated and doubly-reduced species (**RuH<sub>2</sub>**) were studied arising from protonation at these protonation sites.

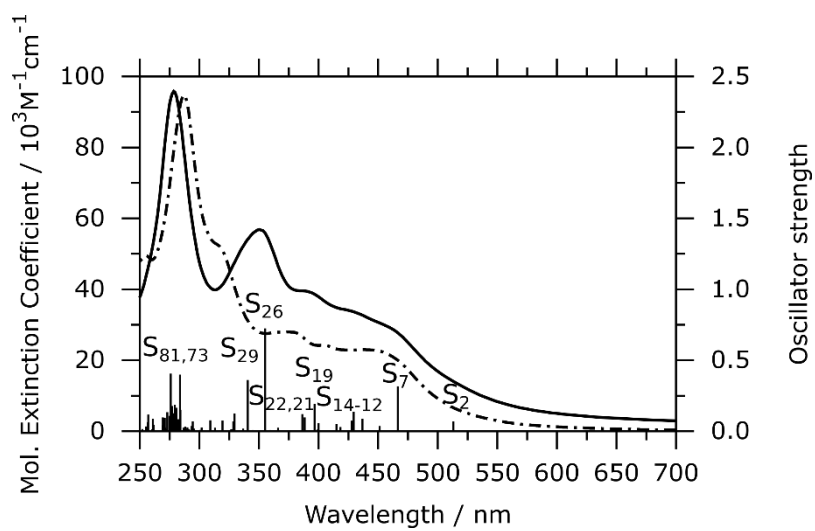
### 1.1 Ru

**Table S1.** Vertical excitation energies ( $\Delta E$ ), electronic character, oscillator strengths ( $f$ ) and spin ( $\langle s^2 \rangle$ ) of the bright singlet-singlet and triplet-triplet excitations contributing to the UVvis absorption (singlet-singlet) and long-lived transient absorption spectrum (negative: singlet-singlet, positive: triplet-triplet) of **Ru** obtained at the TD-DFT level of theory (B3LYP/def2SVP) including GD3BJ dispersion correction and solvent effects (SMD, acetonitrile) by a polarizable continuum model.

		non-reduced (singlet)				
State	Character	$\Delta E / \text{eV}$	$\lambda / \text{nm}$	$f$	$\lambda_{\text{exp}} / \text{nm}$	$\langle s^2 \rangle$
S <sub>2</sub>	MLCT <sub>dppop</sub>	2.42	513	0.0694		0.00
S <sub>7</sub>	ILCT <sub>dppop</sub>	2.66	467	0.3167		0.00
S <sub>9</sub>	MLCT <sub>bpy</sub>	2.75	451	0.0369		0.00
S <sub>12</sub>	MLCT <sub>bpy/dppop</sub>	2.84	437	0.0891	445	0.00
S <sub>13</sub>	MLCT <sub>bpy</sub>	2.89	429	0.1370		0.00
S <sub>14</sub>	MLCT <sub>dppop</sub>	2.90	428	0.0737		0.00
S <sub>16</sub>	MLCT <sub>dppop</sub>	2.99	415	0.0511		0.00
S <sub>17</sub>	MLCT <sub>dppop</sub>	3.10	400	0.0572	405	0.00
S <sub>19</sub>	ILCT <sub>dppop</sub>	3.13	397	0.1936		0.00
S <sub>21</sub>	MLCT <sub>bpy/dppop</sub>	3.19	388	0.0966		0.00
S <sub>22</sub>	ILCT <sub>dppop</sub>	3.21	386	0.1218	381	0.00
S <sub>26</sub>	ILCT <sub>dppop</sub>	3.49	355	0.7250		0.00
S <sub>29</sub>	ILCT <sub>dppop</sub>	3.64	340	0.3604		0.00
S <sub>73</sub>	IL	4.37	284	0.3986		0.00
S <sub>81</sub>	IL	4.49	276	0.4057		0.00
		non-reduced (triplet)				
State	Character	$\Delta E / \text{eV}$	$\lambda / \text{nm}$	$f$	$\lambda_{\text{exp}} / \text{nm}$	$\langle s^2 \rangle$
T <sub>5</sub>	ILCT <sub>dppop</sub>	0.65	1910	0.1117		2.07
T <sub>8</sub>	ILCT <sub>dppop/bpy</sub>	0.80	1543	0.0728		2.06
T <sub>9</sub>	ILCT <sub>dppop</sub>	0.99	1258	0.0602		2.11
T <sub>14</sub>	ILCT <sub>dppop</sub>	1.82	681	0.1214	610	2.13
T <sub>34</sub>	ILCT <sub>dppop</sub>	2.54	488	0.1441	547	2.82
T <sub>41</sub>	ILCT <sub>dppop</sub>	2.86	433	0.1441	547	2.56
T <sub>42</sub>	ILCT <sub>dppop</sub>	2.93	423	0.0792		2.54
T <sub>43</sub>	ILCT <sub>dppop</sub>	3.01	411	0.0731		3.02

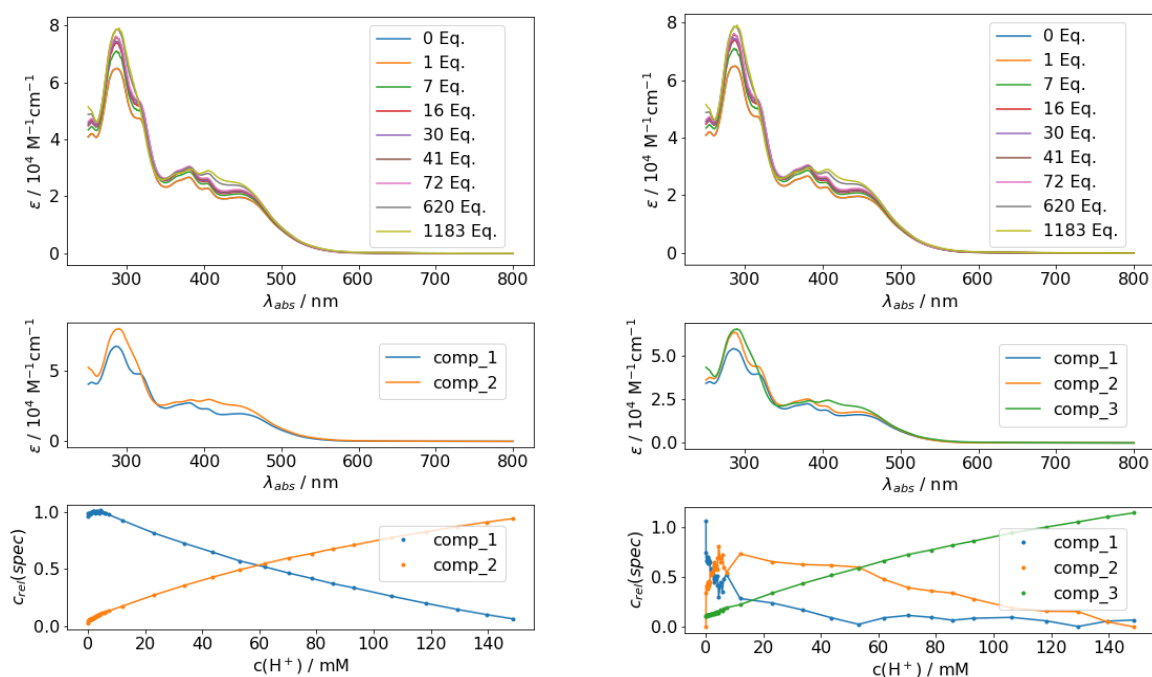
**Table S2.** Charge density differences (CDDs) of some singlet and triplet states involved in the photoexcitation of **Ru** obtained at the TD-DFT level of theory (B3LYP/def2SVP) including GD3BJ dispersion correction and solvent effects (SMD, acetonitrile) by a polarizable continuum model. Excitation goes from red to blue. Spin density of the optimized lowest triplet state ( $T_1$ ), namely a  $^3$ MLCT state.



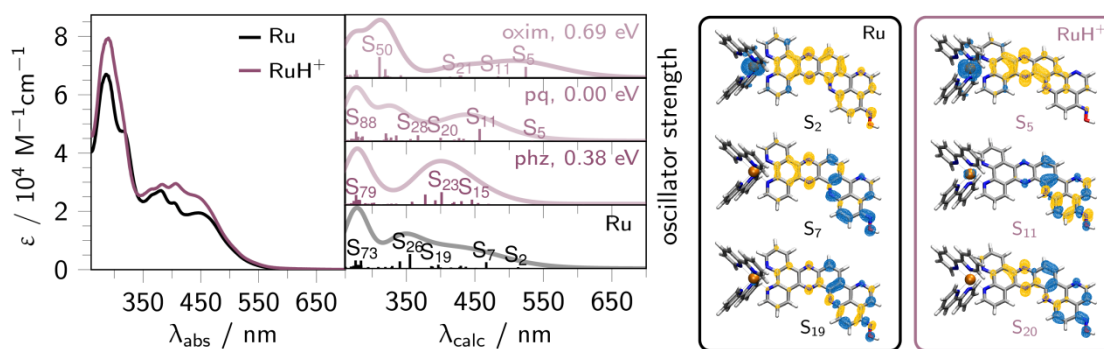


**Figure S2.** TD-DFT simulated absorption spectrum of **Ru**. The obtained vertical transition energies and oscillator strengths are represented by bars, which were spectrally broadened by Gaussian functions (FWHM of 0.2 eV).

## 1.2 RuH<sup>+</sup>

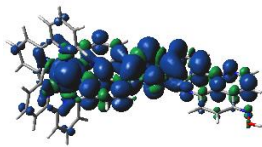
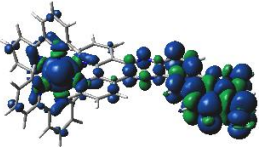
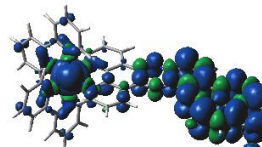


**Figure S3.** *Top* Spectrophotometric acid titration of **Ru** (0.1 mM) with trifluoroacetic acid (addition of 1 up to 1000 molar equivalents). *Bottom:* Multivariate curve resolution least-squares (MCR-LS) results, *i.e.*, extracted spectra and concentrations of **Ru** and **RuH<sup>+</sup>** for a single-step protonation (*left*) and **Ru**, **RuH<sup>+</sup>** and **RuH<sub>2</sub><sup>2+</sup>** for a two-step protonation (*right*). The results indicate that, upon addition of 1000 equivalents of TFA, the complex is singly-protonated in the ground state.



**Figure S4.** *Left:* UVvis absorption spectra of **Ru** and **RuH<sup>+</sup>** in acetonitrile and TD-DFT simulated vertical transition energies and oscillator strengths of **Ru** (black) and three isomers of **RuH<sup>+</sup>** (2 (pq), violet). *Middle:* TD-DFT simulated absorption spectra of **Ru** and three isomers of **RuH<sup>+</sup>**, *i.e.*, when protonation occurs at the dppz, pq or *N*-oxime moiety. The computational results (vertical transition energies and oscillator strengths) are represented by bars. Those bars were spectrally broadened by Gaussian functions (FWHM of 0.2 eV). Their relative energies are given in the simulated spectra (see also Table S3). *Right:* Selected charge density differences of **Ru** and the pq-protonated **RuH<sup>+</sup>** complex (excitation occurs from blue to yellow).

**Table S3.** Relative SCF energies and free energies ( $\Delta G$ ) of three protonation isomers of **Ru**, i.e., upon protonation at the phz (1), pq (2) or *N*-oxim (3) moiety, in their optimized singlet ground state ( $S_0$ ) and lowest triplet state geometry ( $T_1$ ). Spin density distributions of the three protonation isomers in the optimized triplet-state  $^3\text{MLCT}$  manifold ( $T_1$ ).

	$\Delta E / \text{eV}; \Delta G / \text{eV}$		
$S_0$ (FC)	0.38; 0.37	<b>0.00; 0.00</b>	0.69; 0.63
$T_1$ ( $^3\text{MLCT}$ )	1.34; 1.31	1.06; 1.04	1.41; 1.36
spin density			

**Table S4.** Vertical excitation energies ( $\Delta E$ ), electronic character, oscillator strengths ( $f$ ) and spin ( $\langle s^2 \rangle$ ) of the bright singlet-singlet and triplet-triplet excitations contributing to the UVvis absorption (singlet-singlet) and long-lived transient absorption spectrum (negative: singlet-singlet, positive: triplet-triplet) of **RuH<sup>+</sup>** (protonation at the dppz moiety) obtained at the TD-DFT level of theory (B3LYP/def2SVP) including GD3BJ dispersion correction and solvent effects (SMD, acetonitrile) by a polarizable continuum model.

<b>(1) RuH<sup>+</sup> (dppz, singlet)</b>						
State	Character	$\Delta E / \text{eV}$	$\lambda / \text{nm}$	$f$	$\lambda_{\text{exp}} / \text{nm}$	$\langle s^2 \rangle$
S <sub>11</sub>	MLCT <sub>dppop</sub>	2.64	470	0.0482		0.00
S <sub>13</sub>	MLCT <sub>dppop</sub>	2.73	455	0.0916		0.00
S <sub>15</sub>	MLCT <sub>bpy/dppop</sub>	2.78	446	0.2614	445	0.00
S <sub>17</sub>	MLCT <sub>bpy</sub>	2.88	430	0.1843		0.00
S <sub>20</sub>	MLCT <sub>bpy</sub>	2.95	420	0.1398		0.00
S <sub>21</sub>	LLCT/ILCT <sub>bpy/dppop</sub>	2.97	417	0.0777		0.00
S <sub>23</sub>	ILCT <sub>dppop</sub>	3.09	401	0.6364	407	0.00
S <sub>24</sub>	MLCT/ILCT <sub>dppop</sub>	3.16	392	0.2282		0.00
S <sub>26</sub>	ILCT <sub>dppop</sub>	3.28	378	0.5219	383	0.00
<b>(1) RuH<sup>+</sup> (dppz, triplet)</b>						
State	Character	$\Delta E / \text{eV}$	$\lambda / \text{nm}$	$f$	$\lambda_{\text{exp}} / \text{nm}$	$\langle s^2 \rangle$
T <sub>15</sub>	LLCT <sub>dppop/bpy</sub>	2.41	515	0.0585	546	2.05
T <sub>16</sub>	ILCT <sub>dppop</sub>	2.44	508	0.0476	546	2.20
T <sub>26</sub>	ILCT <sub>dppop</sub>	2.85	435	0.2636		3.10
T <sub>30</sub>	ILCT <sub>dppop</sub>	2.98	416	0.0774		3.16
T <sub>31</sub>	ILCT <sub>dppop</sub>	3.03	410	0.1878		2.40
T <sub>34</sub>	LLCT <sub>dppop/bpy</sub>	3.06	405	0.3612		2.59
T <sub>42</sub>	LLCT <sub>dppop/bpy</sub>	3.17	391	0.0586		3.19
T <sub>46</sub>	LMCT/ILCT <sub>dppop</sub>	3.26	380	0.2587		2.23
T <sub>50</sub>	ILCT <sub>dppop</sub>	3.32	373	0.1767		2.44

**Table S5.** Charge density differences (CDDs) of some singlet and triplet states involved in the photo-excitation of  $\text{RuH}^+$  (protonation at the dppz moiety) obtained at the TD-DFT level of theory (B3LYP/def2SVP) including GD3BJ dispersion correction and solvent effects (SMD, acetonitrile) by a polarizable continuum model. Excitation goes from red to blue. Spin density of the optimized lowest triplet state ( $T_1$ ), namely a  $^3\text{MLCT}$  state.

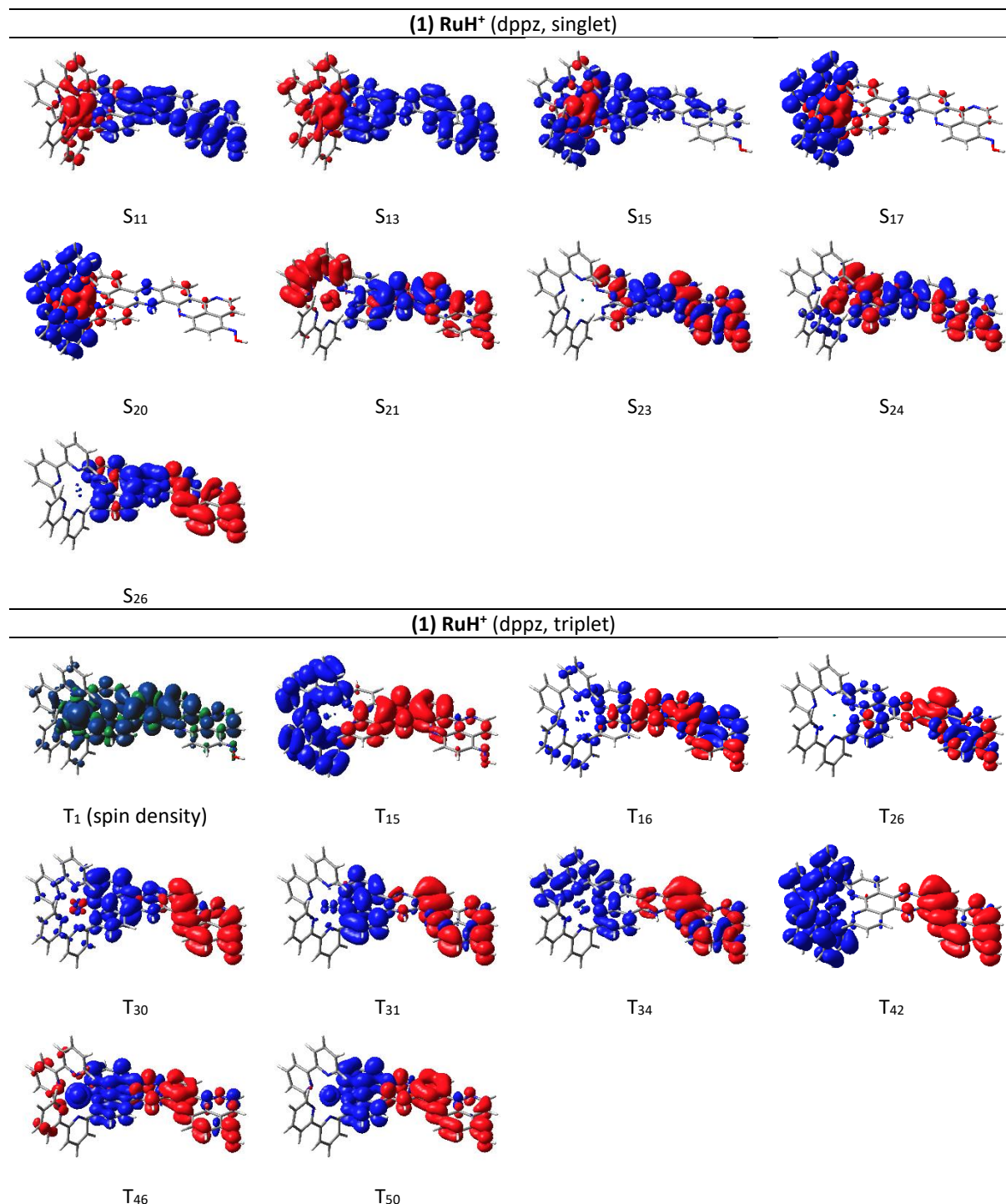




**Table S6.** Vertical excitation energies ( $\Delta E$ ), electronic character, oscillator strengths ( $f$ ) and spin ( $\langle s^2 \rangle$ ) of the bright singlet-singlet and triplet-triplet excitations contributing to the UVvis absorption (singlet-singlet) and long-lived transient absorption spectrum (negative: singlet-singlet, positive: triplet-triplet) of **RuH<sup>+</sup>** (protonation at the pq moiety) obtained at the TD-DFT level of theory (B3LYP/def2SVP) including GD3BJ dispersion correction and solvent effects (SMD, acetonitrile) by a polarizable continuum model.

<b>(2) RuH<sup>+</sup> (pq, singlet)</b>						
State	Character	$\Delta E$ / eV	$\lambda$ / nm	$f$	$\lambda_{\text{exp}}$ / nm	$\langle s^2 \rangle$
S <sub>5</sub>	MLCT <sub>dppop</sub>	2.32	534	0.0451		0.00
S <sub>11</sub>	ILCT <sub>dppop</sub>	2.71	457	0.6145	445	0.00
S <sub>15</sub>	MLCT <sub>bpy/dppop</sub>	2.86	433	0.1162		0.00
S <sub>16</sub>	MLCT <sub>bpy</sub>	2.90	427	0.1512		0.00
S <sub>20</sub>	ILCT <sub>dppop</sub>	3.10	400	0.1700	407	0.00
S <sub>26</sub>	ILCT <sub>dppop</sub>	3.38	367	0.2950	383	0.00
S <sub>28</sub>	ILCT <sub>dppop</sub>	3.48	356	0.1040		0.00
<b>(2) RuH<sup>+</sup> (pq, triplet)</b>						
State	Character	$\Delta E$ / eV	$\lambda$ / nm	$f$	$\lambda_{\text{exp}}$ / nm	$\langle s^2 \rangle$
T <sub>10</sub>	ILCT <sub>dppop</sub>	1.97	630	0.0291	610	3.10
T <sub>16</sub>	ILCT <sub>dppop</sub>	2.42	512	0.1007	546	2.57
T <sub>21</sub>	ILCT <sub>dppop</sub>	2.60	476	0.0334	546	2.85
T <sub>22</sub>	ILCT <sub>dppop</sub>	2.63	472	0.0272	546	2.34
T <sub>25</sub>	ILCT <sub>dppop</sub>	2.69	461	0.0965		2.68
T <sub>26</sub>	ILCT/LLCT <sub>bpy/dppop</sub>	2.72	456	0.0770		3.25
T <sub>40</sub>	ILCT/LMCT <sub>dppop</sub>	3.13	396	0.1219		2.47
T <sub>42</sub>	ILCT <sub>dppop</sub>	3.19	388	0.0525		2.61
T <sub>43</sub>	ILCT <sub>dppop</sub>	3.24	382	0.1536		3.32
T <sub>53</sub>	ILCT <sub>dppop</sub>	3.43	362	0.6007		2.52
T <sub>55</sub>	ILCT <sub>dppop</sub>	3.54	350	0.1715		3.49

**Table S7.** Charge density differences (CDDs) of some singlet and triplet states involved in the photo-excitation of  $\text{RuH}^+$  (protonation at the pq moiety) obtained at the TD-DFT level of theory (B3LYP/def2SVP) including GD3BJ dispersion correction and solvent effects (SMD, acetonitrile) by a polarizable continuum model. Excitation goes from red to blue. Spin density of the optimized lowest triplet state ( $T_1$ ), namely a  $^3\text{MLCT}_{\text{pq}}$  state.

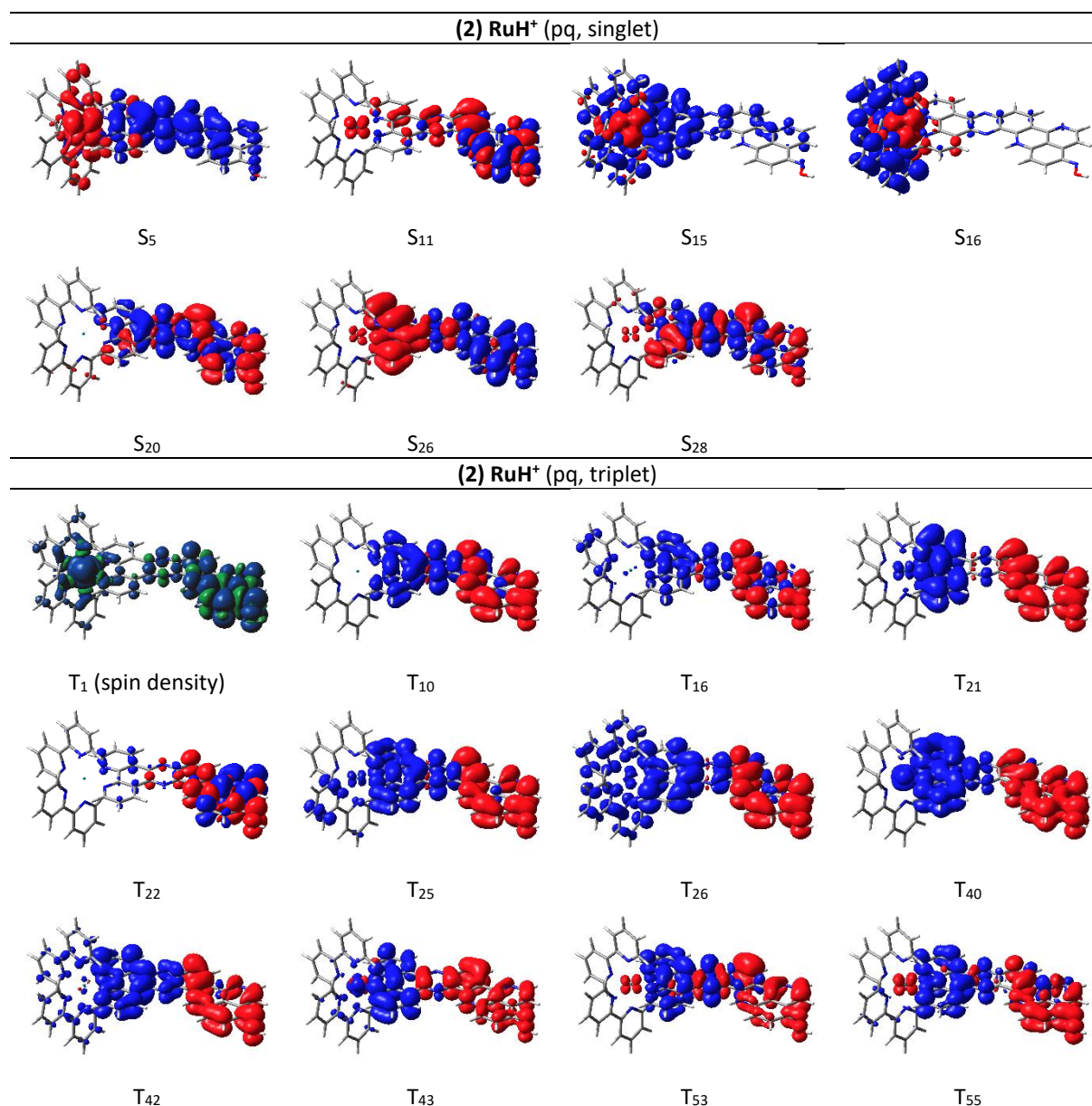
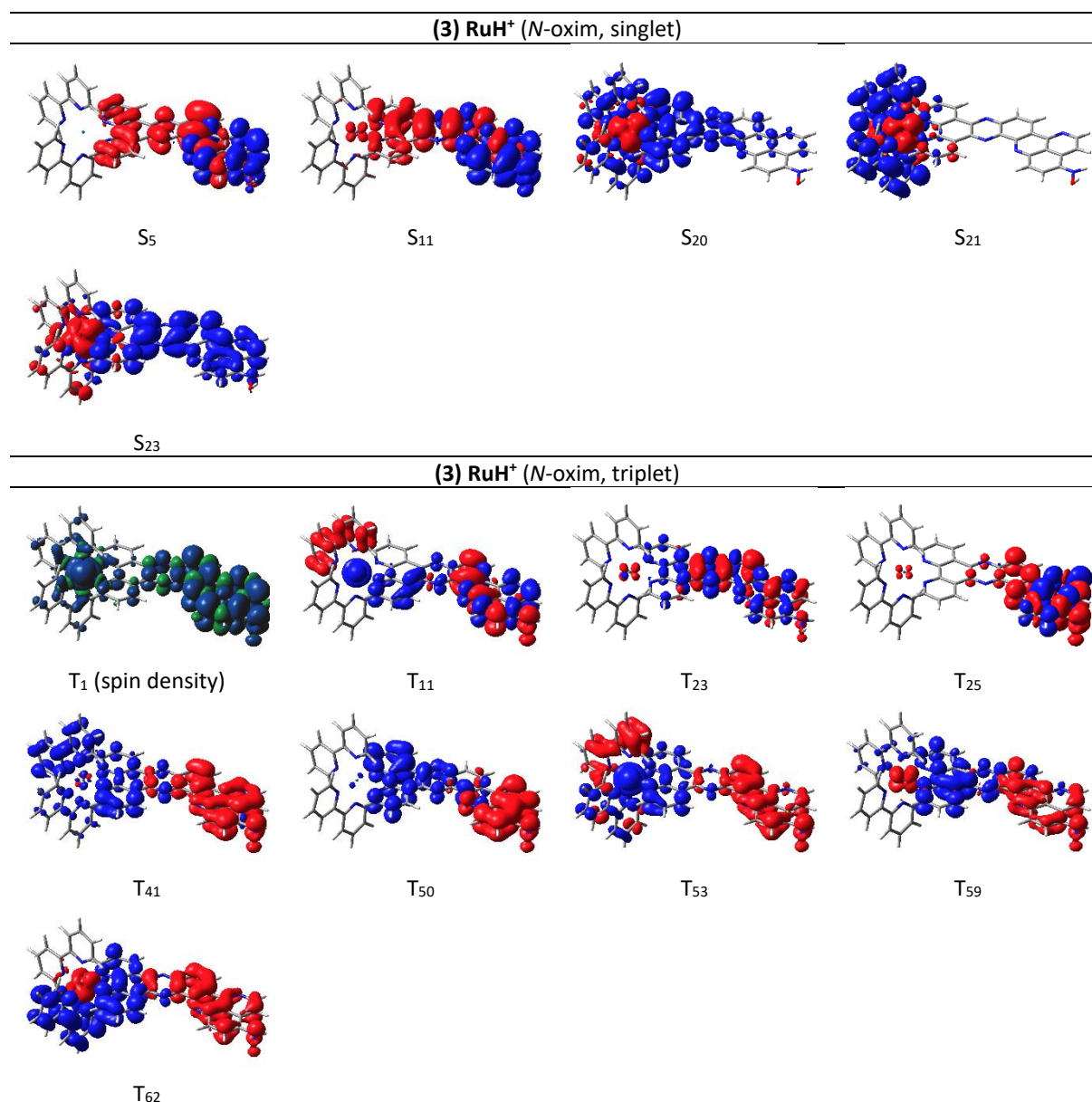


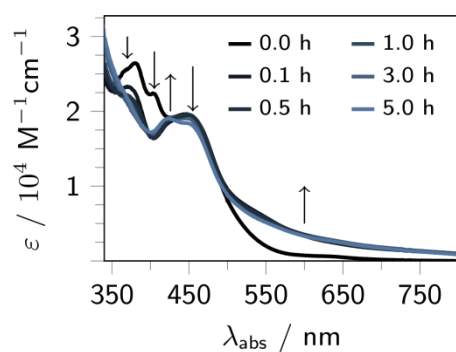
**Table S8.** Vertical excitation energies ( $\Delta E$ ), electronic character, oscillator strengths ( $f$ ) and spin ( $\langle s^2 \rangle$ ) of the bright singlet-singlet and triplet-triplet excitations contributing to the UVvis absorption (singlet-singlet) and long-lived transient absorption spectrum (negative: singlet-singlet, positive: triplet-triplet) of **RuH<sup>+</sup>** (protonation at the *N*-oxim moiety) obtained at the TD-DFT level of theory (B3LYP/def2SVP) including GD3BJ dispersion correction and solvent effects (SMD, acetonitrile) by a polarizable continuum model.

<b>(3) RuH<sup>+</sup> (<i>N</i>-oxim, singlet)</b>						
State	Character	$\Delta E$ / eV	$\lambda$ / nm	$f$	$\lambda_{\text{exp}}$ / nm	$\langle s^2 \rangle$
S <sub>5</sub>	ILCT <sub>dppop</sub>	2.37	524	0.5711		0.00
S <sub>11</sub>	ILCT <sub>dppop</sub>	2.56	484	0.0966		0.00
S <sub>20</sub>	MLCT <sub>bpy/dppop</sub>	2.89	430	0.1387	445	0.00
S <sub>21</sub>	MLCT <sub>bpy</sub>	2.90	428	0.1407		0.00
S <sub>23</sub>	MLCT <sub>dppop</sub>	3.00	414	0.0802	407	0.00
<b>(3) RuH<sup>+</sup> (<i>N</i>-oxim, triplet)</b>						
State	Character	$\Delta E$ / eV	$\lambda$ / nm	$f$	$\lambda_{\text{exp}}$ / nm	$\langle s^2 \rangle$
T <sub>11</sub>	LMCT/ILCT <sub>bpy/dppop</sub>	2.07	599	0.2300	610	2.14
T <sub>23</sub>	ILCT <sub>dppop</sub>	2.82	439	0.2432	546	2.59
T <sub>25</sub>	ILCT <sub>dppop</sub>	2.88	430	0.0415	546	2.08
T <sub>41</sub>	ILCT/LLCT <sub>dppop/bpy</sub>	3.25	382	0.1184		2.92
T <sub>50</sub>	ILCT <sub>dppop</sub>	3.43	362	0.1638		2.20
T <sub>53</sub>	LMCT <sub>dppop/bpy</sub>	3.51	354	0.1134		2.77
T <sub>59</sub>	ILCT <sub>dppop</sub>	3.61	344	0.1200		2.40
T <sub>62</sub>	MLCT/ILCT <sub>dppop/bpy</sub>	3.64	341	0.1619		3.03

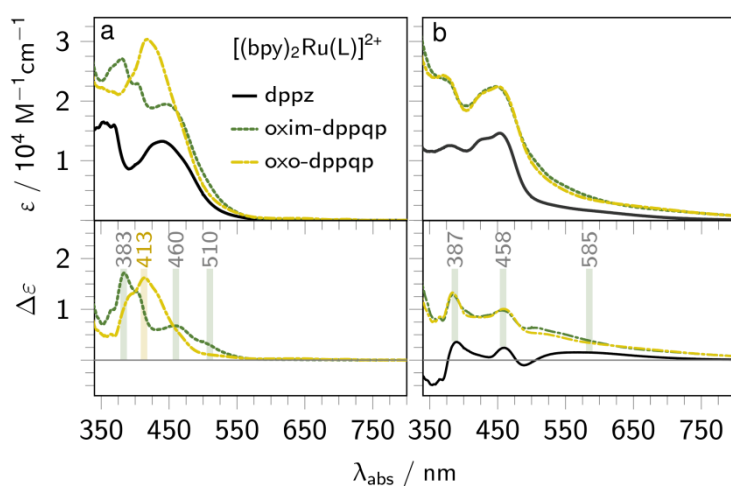
**Table S9.** Charge density differences (CDDs) of some singlet and triplet states involved in the photo-excitation of  $\text{RuH}^+$  (protonation at the *N*-oxim moiety) obtained at the TD-DFT level of theory (B3LYP/def2SVP) including GD3BJ dispersion correction and solvent effects (SMD, acetonitrile) by a polarizable continuum model. Excitation goes from red to blue. Spin density of the optimized lowest triplet state ( $T_1$ ), namely a  $^3\text{MLCT}_{pq}$  state.



### 1.3 RuH<sub>2</sub>

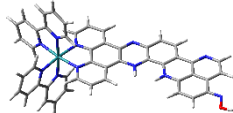
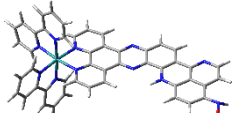
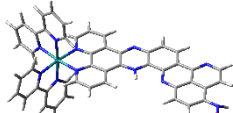
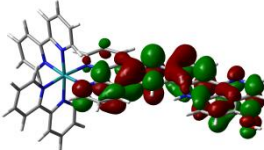
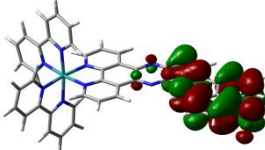
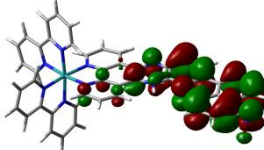


**Figure S5.** UV-vis absorption spectrum of **Ru** in acetonitrile (200  $\mu\text{M}$ ) in the presence of 5000 molar equivalents of triethylamine (0.0 h, black) and upon LED-illumination at 455 nm for 0.1, 0.5, 1.0, 3.0 and 5.0 hours (forming **RuH<sub>2</sub>**). The directions of the spectral changes are indicated by arrows.



**Figure S6.** UV-vis absorption spectra (top row) of  $[(\text{bpy})_2\text{Ru}(\text{dppz})]^{2+}$  (black), **Ru** (green) and  $[(\text{bpy})_2\text{Ru}(\text{oxo-dppqp})]^{2+}$  (yellow) (a) and their photo-reduced derivatives (b) in acetonitrile and difference spectra (bottom) obtained by subtracting the absorption spectrum of the parent complex  $[(\text{bpy})_2\text{Ru}(\text{dppz})]^{2+}$ . The photo-reduced species were formed upon LED-illumination at 455 nm in the presence of a 500 molar equivalents of triethylamine (with respect to the complexes concentration).

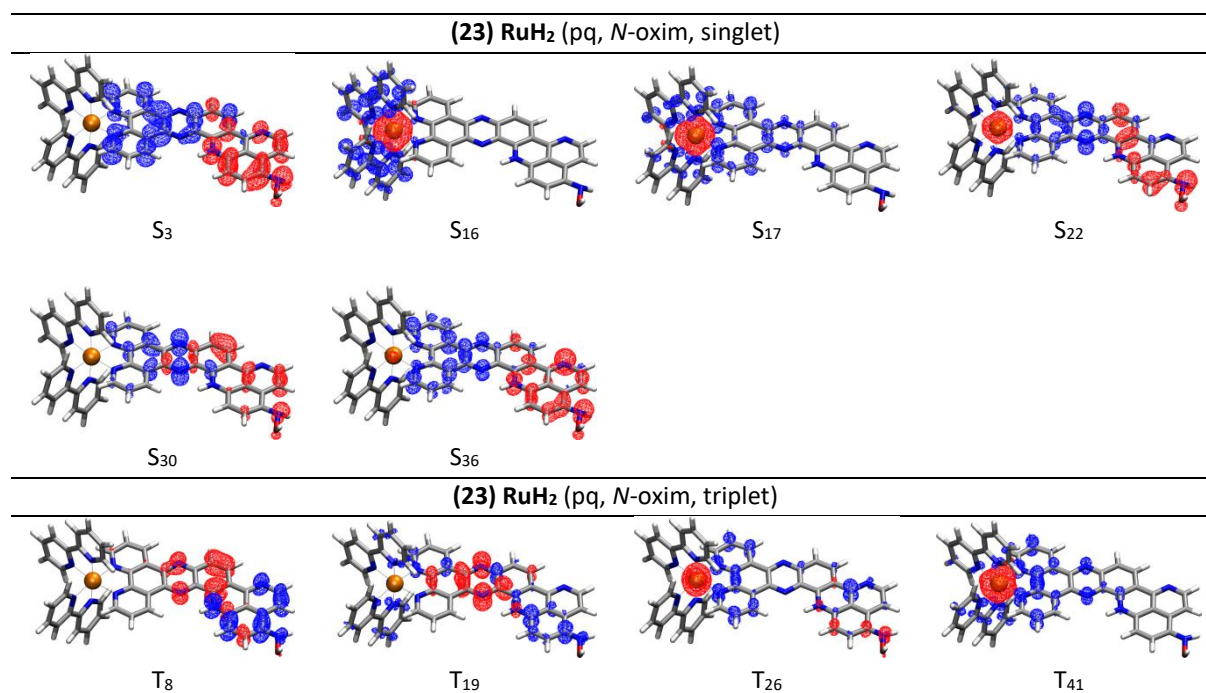
**Table S10.** Relative SCF energies and free energies ( $\Delta G$ ) of three isomers of  $\text{RuH}_2$ , *i.e.*, upon two-electron reduction and protonation at the pq and dppz (12), pq and N-oxim (23), and N-oxim and dppz (13) moieties, in their optimized singlet ground state ( $S_0$ ) and lowest triplet state geometry ( $T_1$ ). Highest unoccupied molecular orbitals (HOMO) of each isomer in the singlet manifold. Spin density distributions of the three protonation isomers in the optimized triplet-state  $^3\text{ILCT}$  manifold ( $T_1$ ).

	$\Delta E / \text{eV}; \Delta G / \text{eV}$		
$S_0$ (FC)	 1.30; 1.26	 <b>0.00; 0.00</b>	 0.90; 0.87
$T_1$ ( $^3\text{ILCT}$ )	 0.87; 0.77	 0.99; 0.87	 0.88; 0.78

**Table S11.** Vertical excitation energies ( $\Delta E$ ), electronic character, oscillator strengths ( $f$ ) and spin ( $\langle s^2 \rangle$ ) of the bright singlet-singlet and triplet-triplet excitations contributing to the UVvis absorption (singlet-singlet) and long-lived transient absorption spectrum (negative: singlet-singlet, positive: triplet-triplet) of **RuH<sub>2</sub>** (protonation at the pq and *N*-oxim moiety) obtained at the TD-DFT level of theory (B3LYP/def2SVP) including GD3BJ dispersion correction and solvent effects (SMD, acetonitrile) by a polarizable continuum model.

<b>(23) RuH<sub>2</sub> (pq, <i>N</i>-oxim, singlet)</b>						
State	Character	$\Delta E$ / eV	$\lambda$ / nm	$f$	$\lambda_{\text{exp}}$ / nm	$\langle s^2 \rangle$
S <sub>3</sub>	ILCT <sub>dppqp</sub>	2.19	567	0.2096		0.00
S <sub>16</sub>	MLCT <sub>bpy</sub>	2.89	429	0.1328		0.00
S <sub>17</sub>	MLCT <sub>bpy</sub> , MLCT <sub>phen</sub>	2.91	427	0.2022		0.00
S <sub>22</sub>	MLCT <sub>dppz</sub> , ILCT <sub>dppqp</sub>	3.18	390	0.1035		0.00
S <sub>30</sub>	ILCT <sub>dppqp</sub>	3.48	356	0.4020		0.00
S <sub>36</sub>	ILCT <sub>dppqp</sub>	3.76	330	0.4755		0.00
<b>(23) RuH<sub>2</sub> (pq, <i>N</i>-oxim, triplet)</b>						
State	Character	$\Delta E$ / eV	$\lambda$ / nm	$f$	$\lambda_{\text{exp}}$ / nm	$\langle s^2 \rangle$
T <sub>8</sub>	$\pi\pi^*_{\text{pq}}$	1.77	702	0.2903	620	2.041
T <sub>19</sub>	ILCT <sub>phz→pq</sub>	2.32	534	0.1388	525	2.099
T <sub>26</sub>	MLCT <sub>phen</sub>	2.49	499	0.1738	480	2.918
T <sub>41</sub>	MLCT <sub>phen</sub>	2.85	435	0.2196	450	2.205

**Table S12.** Charge density differences (CDDs) of some singlet and triplet states involved in the photo-excitation of **RuH<sub>2</sub>** (protonation at the pq and *N*-oxim moiety) obtained at the TD-DFT level of theory (B3LYP/def2SVP) including GD3BJ dispersion correction and solvent effects (SMD, acetonitrile) by a polarizable continuum model. Excitation goes from red to blue.



## 2 Resonance Raman Spectra

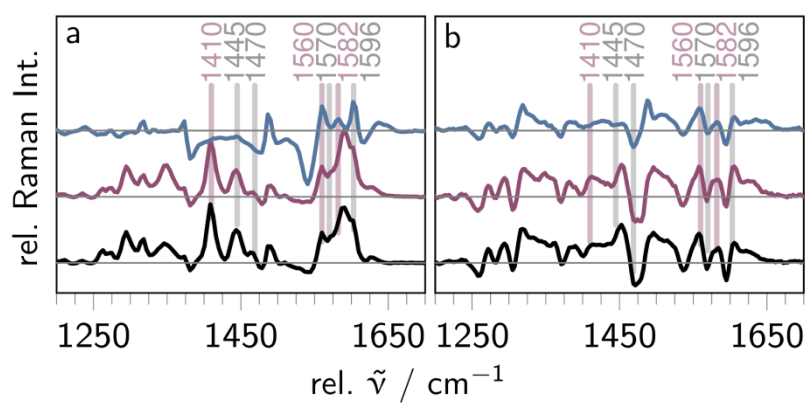


**Figure S7.** Difference resonance Raman (rR) spectra taken between **Ru**, **RuH<sup>+</sup>** and **RuH<sub>2</sub>** and  $[(\text{bpy})_2\text{Ru}(\text{dppz})]^{2+}$  upon 405 nm (**a**) and 473 nm (**b**) excitation in acetonitrile. All spectra were normalized to the solvent band at around 1373  $\text{cm}^{-1}$ . The rR spectra of  $[(\text{bpy})_2\text{Ru}(\text{dppz})]^{2+}$  are subtracted, indicating that modes appearing in the negative signal region are weakened with respect to the parental complex.



### 3 Steady-state and time-resolved emission spectra

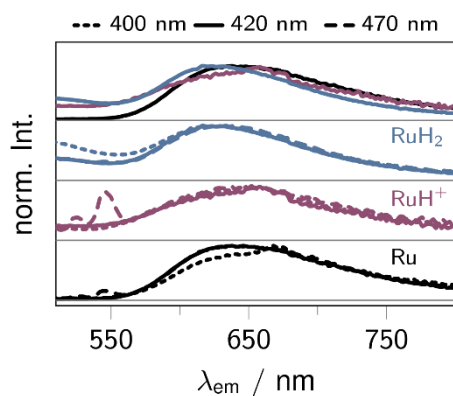


**Figure S8.** Normalized emission spectra of **Ru** (bottom, black), **RuH<sup>+</sup>** (bottom, violet), and **RuH<sub>2</sub>** (top, blue) upon 400 nm (dotted line), 420 nm (solid lines) and 470 nm excitation (dashed lines) in acetonitrile (sample concentration of about 1 μM). For reasons of comparability an overlay of the emission spectra of **Ru**, **RuH<sup>+</sup>**, and **RuH<sub>2</sub>**, collected at 420 nm excitation, is shown in the top panel.

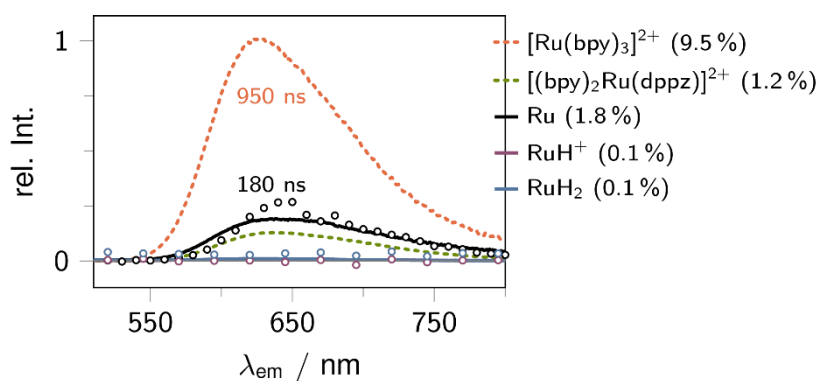


**Figure S9.** Steady-state emission spectra of **Ru** (black, solid line), **RuH<sup>+</sup>** (violet), **RuH<sub>2</sub>** (blue), **[Ru(bpy)<sub>3</sub>]<sup>2+</sup>** (dashed, orange line), and **[(bpy)<sub>2</sub>Ru(dppz)]<sup>2+</sup>** (dashed, green line) upon 420 nm excitation in acetonitrile. The spectra were collected at the same sample concentration, *i.e.*, 1 μM and are normalized with respect to the spectrum of **[Ru(bpy)<sub>3</sub>]<sup>2+</sup>** (highest emission quantum yield of 9.5%). The emission quantum yields of the samples are given in parentheses and were determined relative to **[Ru(bpy)<sub>3</sub>]<sup>2+</sup>**. The blue and violet symbols show the signal detected 50 ns upon excitation of **RuH<sup>+</sup>** and **RuH<sub>2</sub>**. The black symbols correspond to the emission spectrum associated with the mono-exponential decay (180 ns) of the emission signals of **Ru**.

## 4 Time-resolved emission and transient absorption data

### 4.1 Characterization of the long-lived excited state

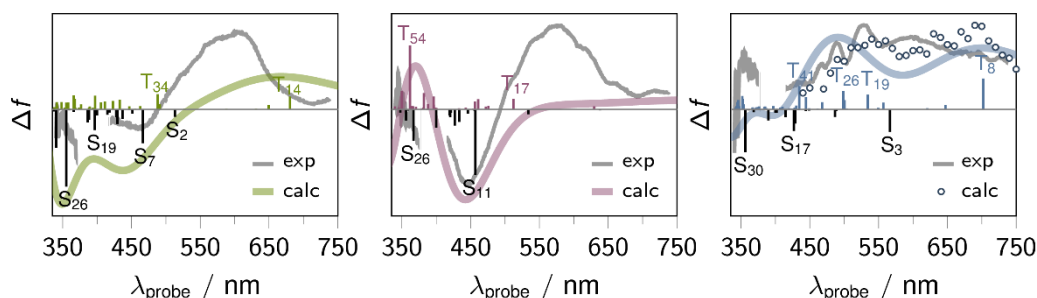


**Figure S10.** Simulated transient absorption spectra (colored spectra) of **Ru** (green), **RuH<sup>+</sup>** (violet, isomer: **2**) and **RuH<sub>2</sub>** (blue, isomer: **23**) obtained for a  $S_0$  to  $T_1$  excitation. The respective simulated triplet state minima correspond to a  ${}^3\text{MLCT}_{\text{pq}}$  (**Ru** and **RuH<sup>+</sup>**, see **Table S2** and **S3**) or  ${}^3\pi\pi^*$  state (**RuH<sub>2</sub>**, see **Table S10**), respectively. The predicted vertical transition energies and oscillator strengths in the triplet (colored) and singlet (black) sphere are indicated by bars. For comparison to the experimental results the spectrum associated with the thermally equilibrated  ${}^3\text{MLCT}_{\text{pq}}$  (**Ru** and **RuH<sup>+</sup>**) or  ${}^3\pi\pi^*$  (**RuH<sub>2</sub>**) excited state is shown in gray.

### 4.2 Photoinduced dynamics

For target modelling the fs-TA data of **Ru** and **RuH<sup>+</sup>** the following differential equations (1)-(4) were numerically integrated. The respective spectrum of each component (excited state, namely 1:  ${}^1\text{MLCT}$ , 2:  ${}^1\pi\pi^*$ , 3:  ${}^3\text{MLCT}_{\text{pq}}$ , 4:  ${}^3\pi\pi^*$ ) is obtained from the pre-exponential factors of the global fit at each studied probe wavelength:

$${}^1\text{MLCT:} \quad \frac{dc(1)}{dt} = -k_1 \cdot c(1) \quad (1)$$

$${}^1\pi\pi^*: \quad \frac{dc(2)}{dt} = -k_2 \cdot c(2) \quad (2)$$

$${}^3\text{MLCT}_{\text{pq}}: \quad \frac{dc(3)}{dt} = k_1 \cdot c(1) - k_3 \cdot c(3) \quad (3)$$

$${}^3\pi\pi^*: \quad \frac{dc(4)}{dt} = k_2 \cdot c(2) - k_4 \cdot c(4) \quad (4)$$

For modelling the fs-TA data of **RuH<sub>2</sub>**, the following rate equations (5)-(7) were numerically solved, involving the three states  ${}^1\text{MLCT}$ ,  ${}^1\pi\pi^*$ , and  ${}^3\pi\pi^*$ .

$${}^1\text{MLCT:} \quad \frac{dc(1)}{dt} = -k_1 \cdot c(1) \quad (5)$$

$${}^1\pi\pi^*: \quad \frac{dc(2)}{dt} = -k_2 \cdot c(2) \quad (6)$$

$${}^3\pi\pi^*: \quad \frac{dc(3)}{dt} = k_1 \cdot c(1) + k_2 \cdot c(2) - k_3 \cdot c(3) \quad (7)$$

The respective species associated spectra obtained by the target models are summarized in Figure S11. All global and target analysis steps were performed using the KiMoPack software.

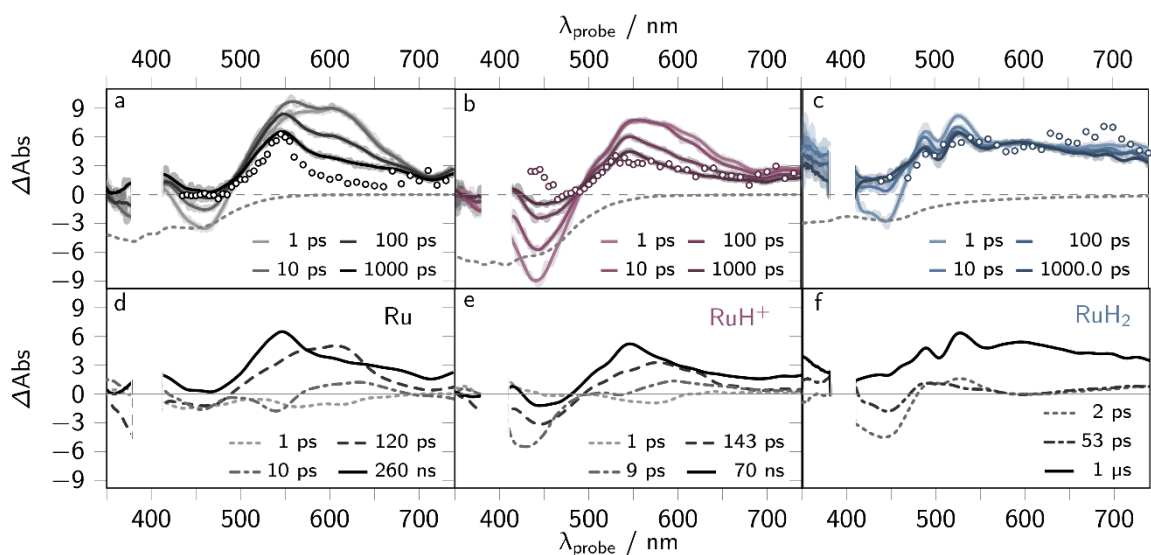


**Figure S11.** Ultrafast transient absorption (a - c) and decay associated spectra (d - f) of **Ru** (a and d), **RuH<sup>+</sup>** (b and e) and **RuH<sub>2</sub>** (c and f) upon excitation at 400 nm (0.4 mW, excitation densities of around 5 %) in acetonitrile. The symbols in panel a, b, and c show the scaled, long-lived spectrum obtained from nanosecond-time-resolved transient absorption spectroscopy upon 420 nm excitation (0.5 mW). The characteristic time constants beyond 2 ns were obtained from nanosecond-time-resolved TA spectroscopy.